Thomas J. Vogl, MD
Nasreddin D. Abolmaali, MD
Thomas Diebold, MD
Kerstin Engelmann
Mehtap Ay
Selami Dogan, MD
Gerhardt Wimmer-Greinecker, MD
Anton Moritz, MD
Christopher Herzog, MD

Index terms:
Angiography, 51.124
Computed tomography (CT), angiography, 51.12116
Computed tomography (CT), multi–detector row
Computed tomography (CT), three-dimensional, 51.12117
Coronary vessels, CT
Heart, CT, 51.12116, 51.12117

Published online before print
10.1148/radiol.2231010515
Radiology 2002; 223:212–220

Abbreviations:
ECG = electrocardiographic
HRS = hemodynamically relevant stenoses
LCA = left coronary artery
LCX = left circumflex
MPR = multiplanar reformation
RCA = right coronary artery
3D = three dimensional
VE = virtual endoscopy

[1] From the Institute for Diagnostic and Interventional Radiology (T.J.V., N.D.A., T.D., K.E., M.A., C.H.) and Department of Thoracic and Cardiovascular Surgery (S.D., G.W.G., A.M.), J. W. Goethe-University Frankfurt, Theodor-Stern-Kai 7, 60590 Frankfurt, Germany. Received February 28, 2001; revision requested April 2; revision received July 2; accepted September 7. **Address correspondence to** C.H. (e-mail: *c.herzog@em.uni-frankfurt.de*).

Author contributions:
Guarantor of integrity of entire study, T.J.V.; study concepts, T.J.V., C.H.; study design, N.D.A., T.D.; literature research, K.E., M.A.; clinical studies, T.J.V., N.D.A.; experimental studies, C.H., G.W.G.; data acquisition, S.D., M.A.; data analysis/interpretation, K.E., N.D.A.; statistical analysis, A.M.; manuscript preparation, G.W.G., T.J.V.; manuscript definition of intellectual content, T.D., T.J.V.; manuscript editing, C.H., N.D.A.; manuscript revision/review, N.D.A., T.D.; manuscript final version approval, T.J.V., C.H.

Techniques for the Detection of Coronary Atherosclerosis: Multi–detector Row CT Coronary Angiography[1]

PURPOSE: To investigate the accuracy of different computed tomographic (CT) reformation techniques in assessing the coronary arteries.

MATERIALS AND METHODS: Sixty-four patients undergoing both multi–detector row CT and invasive coronary angiography were consecutively included in a retrospective study. CT scans were obtained with collimation of 4 × 1 mm, pitch of 1.5, and rotation time of 500 msec. Retrospective electrocardiographic gating was used for image reconstruction, with 1.25-mm section thickness and 0.5-mm increment. The CT data set of each patient was evaluated by independent observers using transverse scanning, virtual endoscopic, and three-dimensional reformation and multiplanar reformation.

RESULTS: Hemodynamically relevant stenoses (>50%) were detected with highest sensitivity at transverse scanning (58 of 79 [73.4%] stenoses), followed by virtual endoscopic (38 of 79 [48.1%] stenoses) and three-dimensional reformation (34 of 79 [43.0%] stenoses), and multiplanar reformation (37 of 79 [46.8%] stenoses). Atherosclerotic plaques were identified with comparable sensitivities at transverse scanning (143 of 218 plaques [65.6%]) and at three-dimensional (139 of 218 [63.8%] plaques) and virtual endoscopic reformation (136 of 218 [62.4%] plaques). Multiplanar reformation had distinctly poorer results (217 of 218 [58.3%] plaques). Combined interpretation with all four techniques increased sensitivity to 74.7% (59 of 79) for stenosis and 71.6% (156 of 218) for atherosclerosis. Calculated overall specificity was 91.4% or greater. Sufficient vascular evaluation was possible only in vessels larger than 1.6 mm in diameter. Thus, even in patients with heart rates below 60 bpm, only 80.0% of all coronary segments could be visualized, while at higher frequencies, visibility decreased to 66.2%.

CONCLUSION: Although multi–detector row CT is a favorable alternative procedure in evaluating coronary arteries, its clinical value still is restricted to low heart rates and proximal coronary arterial segments.

With the advent of multi–detector row technology combined with subsecond rotation and retrospective electrocardiographic (ECG) gating, computed tomography (CT) has become a clinically important noninvasive diagnostic technique in cardiac imaging (1,2). For the first time, high-resolution CT angiography of the coronary arteries may be performed under reproducible clinical and technical circumstances. As compared with conventional single-section CT, not only is acquisition time markedly decreased, but z-plane and in-plane resolution are also substantially improved (3,4). Thus, even with use of narrow collimation, the complete heart volume may easily be scanned in one breath hold.

Although transverse scanning normally represents the clinical reference standard for detailed image analysis, in coronary imaging its diagnostic value is restricted by vascular diameters averaging only 3 mm and three-dimensional (3D) spreading of the vessels. Consequently, vascular sections are often displayed at an unfavorable cutting angle or are affected by partial volume effects (5).

Use of additional visualization techniques may therefore help reduce these disadvan-

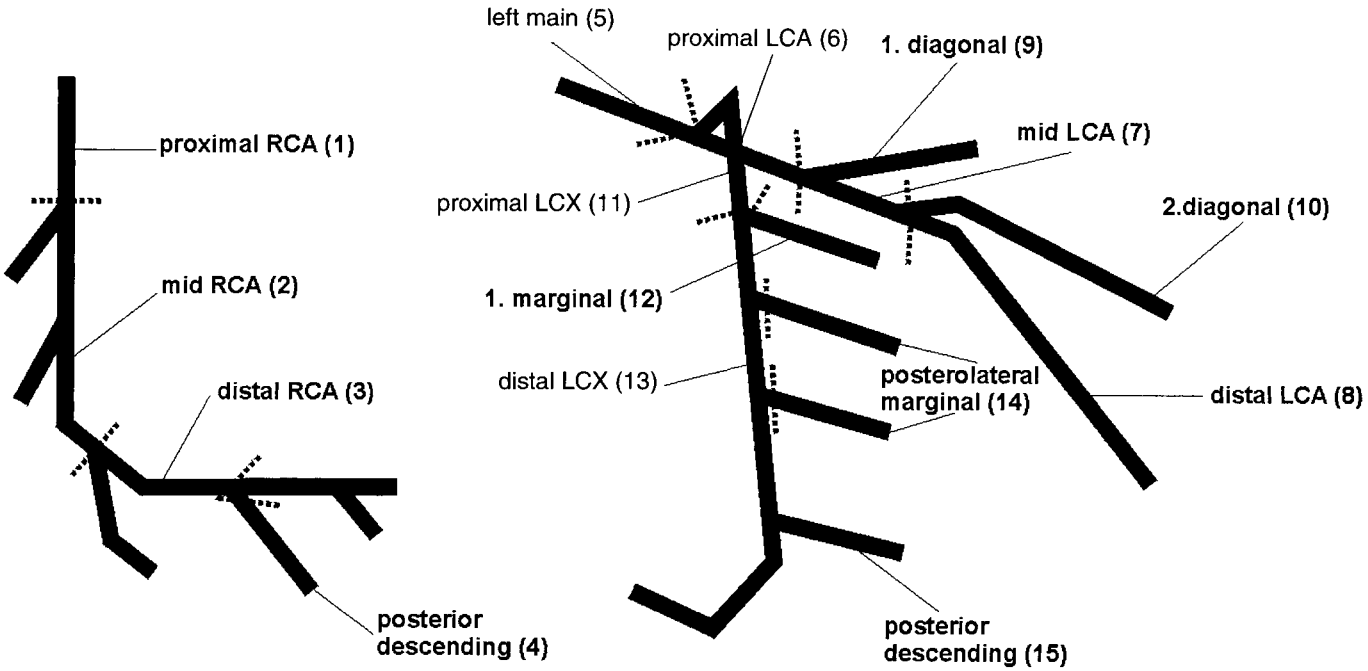

Figure 1. Coronary segments according to AHA classification (7), and subdivision of coronary arteries into 15 segments. Segments 1–4 correspond to RCA; segment 5, to the left main branch, segments 6–10, to the LCA; and segments 11–15, to the LCX. *1.* = first, *2.* = second.

TABLE 1
Visibility of Coronary Arteries in Correlation to Heart Rate and Imaging Technique Applied

Vessels and Imaging Technique	<60 bpm		60–70 bpm		>70 bpm	
RCA						
3D reformation	69.2	(36/52)	57.5	(48/80)	55.6	(69/124)
Virtual endoscopic reformation	53.8	(28/52)	36.3	(29/80)	34.7	(43/124)
MPR	44.2	(23/52)	30.0	(24/80)	30.6	(38/124)
Transverse scanning reformation	82.7	(43/52)	72.5	(58/80)	62.1	(77/124)
LCA						
3D reformation	91.0	(71/78)	86.7	(104/120)	80.0	(149/186)
Virtual endoscopic reformation	74.4	(58/78)	64.1	(77/120)	40.8	(76/186)
MPR	84.6	(66/78)	72.5	(87/120)	65.6	(122/186)
Transverse scanning reformation	91.0	(71/78)	90.0	(108/120)	83.9	(156/186)
LCX						
3D reformation	67.7	(44/65)	56.0	(56/100)	47.1	(73/155)
Virtual endoscopic reformation	41.5	(27/65)	34.0	(34/100)	32.3	(50/155)
MPR	47.7	(31/65)	37.0	(37/100)	30.2	(47/155)
Transverse scanning reformation	64.6	(42/65)	57.0	(57/100)	48.4	(75/155)
Total						
3D reformation	76.9	(150/195)	68.3	(208/300)	62.6	(291/465)
Virtual endoscopic reformation	53.8	(105/195)	46.7	(140/300)	36.3	(169/465)
MPR	63.5	(124/195)	49.3	(148/300)	44.5	(207/465)
Transverse scanning reformation	80.0	(156/195)	74.3	(223/300)	66.2	(308/465)

Note.—Data are percentages. Numbers in parentheses are numbers of coronary arteries.

tages, particularly since both high in-plane and temporal resolution generally improve image quality for 3D modes such as multiplanar, volume-rendered, and virtual endoscopic (VE) reformation.

The purpose of this study was therefore to investigate the accuracy of such complementary visualization techniques in noninvasive assessment of the coronary arteries.

MATERIALS AND METHODS

Patients

We studied retrospectively 64 patients (36 men and 28 women) who had consecutively undergone multi–detector row CT, as well as invasive coronary angiography, over an 8-month period. The average time between the two examinations was 11 days (range, 2–16 days); mean patient age was 56.4 years (range, 46–79 years). Mean patient heart rate was 64.2 beats per minute (bpm) (range, 40.4–87.0 bpm). Twenty-nine examinations were performed in patients presenting with signs of unstable angina pectoris within the scope of preventive diagnostics; 35 patients were studied before total endoscopic coro-

nary artery bypass. Our institutional review board did not require its approval or informed consent for the study.

Data Acquisition

All CT scans were obtained by using a multi–detector row spiral scanner (Somatom Plus 4 VolumeZoom WIP Version VA 20; Siemens, Forchheim, Germany). Patients with heart rates higher than 70 bpm had previously received a short-lasting beta-blocker (100 mg, 1 mL per 10 kilograms of body weight, esmolol hydrochloride, Brevibloc; Baxter, Unterschleissheim, Germany) to obtain rates of 60 bpm or less. However, as medical treatment often did not produce any effect, in some patients, heart rates higher than 70 bpm were observed. A standard scanning protocol was applied, with 4 × 1-mm section collimation, 1.5-mm table feed per rotation, and 500-msec rotation time. Because of 180° linear interpolation, exposure time was minimized to 250 msec. Each scan was obtained at 140 kV and 300 mAs. All patients received 140–160 mL of a noniodine contrast medium (ioprovid, Ultravist; Schering, Berlin, Germany) through an 18-gauge intravenous antecubital catheter infused at a flow rate of 3.5 mL/sec. Start delay was calculated by using a test bolus technique (30 mL contrast medium at a flow rate of 3.5 mL/sec) in the ascending aorta.

Image Reconstruction and Reformation Techniques

Image reconstruction was performed with 1.25-mm effective section thickness, 0.5-mm increment, and B30 kernel, a medium soft-tissue kernel. All reconstruction was performed by using retrospective ECG gating. For this technique, an ECG file recorded simultaneously in the course of the scanning procedure was assigned to the data set retrospectively, thus allowing reconstruction of the scanned volume during any phase of the cardiac cycle (4). Depending on the heart rate, two reconstruction algorithms were applied: a single-segmental reconstruction (<65 bpm) and an adaptive-two-segmental reconstruction (>65 bpm). To reconstruct each 1.25-mm section, single-segmental reconstruction required data from only one rotation; adaptive two-segmental reconstruction, from at least two. Because scanner geometry temporal resolution for adaptive two-segmental reconstruction amounted to 125 msec, for single-segmental reconstruction it did not exceed 250 msec. Each data set was reconstructed seven times before the next R-peak, in intervals of 50 msec (time frame, 650–350 msec). Subsequently, an optimal reconstruction interval was determined for each coronary artery (6).

All data sets were displayed by using four visualization techniques: transverse scanning, 3D and VE reformation, and multiplanar reformation (MPR). Transverse scans were analyzed at a workstation (Wizzard; Siemens), and 3D and VE reformations and MPRs were analyzed at another workstation (3D Virtuoso; Siemens).

Three-dimensional and VE reformation were performed by using a volume-rendering technique. VE navigation was performed manually by one of the observers (C.H.). By using the centerline of VE as a reference line, all MPRs were obtained strictly orthogonally through the

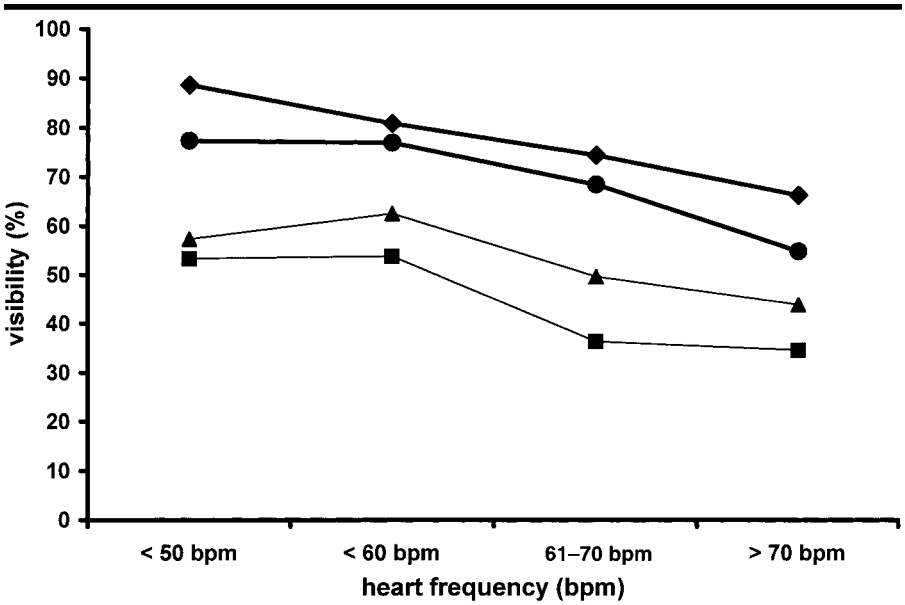

Figure 2. Graph shows visibility of coronary arteries, depending on heart rate and imaging technique (● = 3D reformation, ■ = VE reformation, ▲ = MPR; and ◆ = transverse scanning). The best visibility was obtained at heart rates below approximately 60 bpm. Transverse scans proved least irritable against cardiac motion, since, even at heart rates higher than 70 bpm, overall visibility still amounted to 66.2%.

TABLE 2
Visibility of Coronary Segments in Dependence on Heart Rate Transverse Scanning Results

Vessels and Segments	≤60 bpm		≤70 bpm		>70 bpm	
RCA						
1	100.0	(13/13)	95.0	(19/20)	87.1	(27/31)
2	69.3	(9/13)	55.0	(11/20)	32.3	(10/31)
3	76.9	(10/13)	65.0	(13/20)	54.8	(17/31)
4	84.6	(11/13)	75.0	(15/20)	74.2	(23/31)
LM						
5	100.0	(13/13)	100.0	(20/20)	100.0	(31/31)
LCA						
6	100.0	(13/13)	100.0	(20/20)	96.8	(30/31)
7	100.0	(13/13)	100.0	(20/20)	96.7	(30/31)
8	84.6	(11/13)	80.0	(16/20)	74.2	(23/31)
9	100.0	(13/13)	95.0	(19/20)	77.4	(24/31)
10	69.3	(9/13)	65.0	(13/20)	58.0	(18/31)
LCX						
11	100.0	(13/13)	95.0	(19/20)	87.1	(27/31)
12	76.9	(10/13)	65.0	(13/20)	54.8	(17/31)
13	53.8	(7/13)	45.0	(9/20)	35.5	(11/31)
14	53.8	(7/13)	45.0	(9/20)	32.3	(10/31)
15	38.5	(5/13)	35.0	(7/20)	32.3	(10/31)

Note.—Data are percentages. Numbers in parentheses are numbers of coronary arterial segments.

TABLE 3
Sensitivity and Specificity of CT Coronary Angiography for Detection of Atherosclerosis and HRS (>50%)

Location	Atherosclerosis					HRS				
	3D	VE	MPR	TR	Combined	3D	VE	MPR	TR	Combined
RCA										
Sensitivity	50.1 (29/57)	63.2 (36/57)	47.4 (27/57)	68.4 (39/57)	71.9 (41/57)	28.6 (4/14)	28.6 (4/14)	21.4 (3/14)	57.1 (8/14)	57.1 (8/14)
Specificity	98.4 (251/256)	93.8 (240/256)	93.8 (240/256)	96.0 (246/256)	95.7 (245/256)	99.2 (254/256)	99.2 (254/256)	99.2 (254/256)	100.0 (256/256)	100.0 (256/256)
LCA										
Sensitivity	79.6 (78/98)	77.6 (76/98)	75.5 (74/98)	86.7 (85/98)	87.8 (86/98)	53.2 (25/47)	66.0 (31/47)	61.7 (29/47)	85.1 (40/47)	85.1 (40/47)
Specificity	92.9 (357/384)	87.8 (337/384)	91.7 (352/384)	87.2 (335/384)	89.3 (343/384)	95.8 (368/384)	97.5 (374/384)	97.6 (375/384)	98.6 (379/384)	98.6 (379/384)
LCX										
Sensitivity	50.8 (32/63)	34.9 (22/63)	39.7 (25/63)	57.1 (36/63)	57.1 (36/63)	11.1 (2/18)	22.2 (4/18)	22.2 (4/18)	55.5 (10/18)	55.5 (10/18)
Specificity	96.0 (307/384)	93.8 (300/320)	94.3 (302/320)	98.1 (314/320)	98.1 (314/320)	98.4 (316/320)	98.7 (316/320)	98.1 (314/320)	100.0 (320/320)	100.0 (320/320)
Total										
Sensitivity	63.8 (139/218)	62.4 (136/218)	58.3 (127/218)	65.6 (143/218)	71.6 (156/218)	43.0 (34/79)	48.1 (38/79)	46.8 (37/79)	73.4 (58/79)	74.7 (59/79)
Specificity	95.3 (915/960)	91.4 (877/960)	93.2 (895/960)	93.4 (897/960)	95.5 (902/960)	97.7 (938/960)	98.4 (944/960)	98.2 (943/960)	99.5 (955/960)	99.3 (955/960)

Note.—Data are percentages. Numbers in parentheses are numbers of stenoses or atherosclerotic plaques. TR = transverse scanning.

vessel's course. Transverse scans and MPRs were displayed on a 512 × 512 matrix; 3D and VE reformations, on a 256 × 256 matrix.

Image Evaluation

Evaluation of the coronary arteries was performed according to the classification of the American Heart Association, or AHA, which differentiates between 15 segments (7) (Fig 1). After initial blinding, each dataset was examined by three observers (T.J.V., C.H., N.D.A.) in each case, leading to a final consensus decision.

Images obtained with the four visualization techniques—transverse scanning, 3D and VE reformation, and MPR—were examined in four separate readings. Additionally, in a fifth reading, images obtained by combining all techniques were interpreted. Each observer rated each patient and visualization technique. A delay of at least 7 days was observed between individual evaluations to avoid recall bias.

All findings were compared with corresponding previously blinded coronary angiograms, which had been evaluated previously by the same three observers (T.J.V., C.H., N.D.A.), without knowledge of the CT results. All observers were trained in the evaluation of this technique as the current reference standard.

Coronary angiography had been performed with different technical systems by using the Judkins technique. At least four views of the left coronary arterial (LCA) system and two views of the right coronary arterial (RCA) system were analyzed. Segmental evaluation was performed according to AHA classification (Fig 1). Criteria to be analyzed were *(a)* visibility of the coronary arteries, depending on heart rate; and *(b)* extent of atherosclerosis.

Visibility influenced whether vascular structures could be evaluated correctly or only insufficiently. Thus, only sections showing sharp delimitation from surrounding structures; a nearly artifact-free course of the segment, with less blurring, even in its peripheral sections; and sufficient delimitation between vascular lumen and wall were defined as "visible." Visibility of each coronary segment was explored solely on transverse scans, whereas visibility of the vascular branches as a whole, that is, the RCA (segments 1–4), left main coronary artery (segment 5), LCA (segments 5–10), and left circumflex (LCX) coronary artery (segments 11–15) was examined for each of the four visualization techniques (transverse scanning, MPR, and 3D and VE reformation). For discussion of possible dependence on heart rate, all patients were additionally subdivided into four groups: all patients (n = 64), patients with a heart rate of 60 bpm or less (n = 13), patients with a heart rate of 61–70 bpm (n = 20), and patients with a heart rate of more than 70 bpm (n = 31).

In each coronary arterial segment, the extent of atherosclerosis was determined by differentiating between atherosclerosis and hemodynamically relevant stenosis (HRS). Atherosclerosis was defined as slight to moderate wall change, without substantial narrowing of the vessel (<50%), whereas HRS was defined as substantial wall irregularity, with more than 50% vascular narrowing. The degree of stenosis on transverse scans and MPRs was measured by using an automated distance-measuring tool; on 3D and VE reformations, it could only be estimated. For invasive coronary angiography, a stenosis-grading tool (CMS-View; Medis, Leiden, the Netherlands) with automatic distance and scale calibration was used to determine the amount of stenosis.

Statistical Analysis

Visibility of single coronary arterial segments and main vascular branches was calculated in proportion to the maximum number of segments present, that is, 64 for each of the 15 segments, 256 for the RCA, 384 for the LCA, and 320 for the LCX. Results obtained from invasive coronary angiography served as the reference standard.

The sensitivities and specificities of transverse scans, 3D and VE reformations, and MPRs in the detection of ath-

erosclerosis and high-grade stenoses were calculated in correlation to the number of lesions detected by using the invasive technique as the current reference standard. Because of the low number of lesions per segment, calculation was not performed for each segment separately but for those segments that together built one vascular branch, that is, segments 1–4 for the RCA, segments 5–10 for the LCA, and segments 11–15 for the LCX. Additional total sensitivity and specificity were calculated by considering all 15 coronary arterial segments.

RESULTS

Visibility of Coronary Arteries and Segments

The best visibility was with transverse scanning, which proved less sensitive to cardiac movement than did other visualization techniques (Table 1). In comparison, at heart rates greater than 70 bpm, 3D reformation (62.6%), MPR (44.5%), and VE reformation (36.3%) showed markedly decreased equivalents, whereas visibility of the complete coronary tree at transverse scanning still was 66.2% (Table 1). Nevertheless, visibility with all four techniques decreased with increasing frequencies (Fig 2).

With focus on the three main branches for transverse scanning, the following visibilities were noted: LCA: 91.0% (≤60 bpm), 90.0% (≤70 bpm), and 83.9% (>70 bpm); RCA: 82.7% (≤60 bpm), 72.5% (≤70 bpm), and 62.1% (61–70 bpm); and LCX: 64.6% (≤60 bpm), 57.0% (≤70 bpm), and 48.4% (>70 bpm) (Table 1).

Vessels smaller than 1.6 mm in diameter generally could not be judged properly with any visualization technique. For VE reformation and MPR, visibility was limited to vessels larger than 1.8 mm in diameter. A dependence between visibility and vascular diameter or heart rate was obvious. Thus, visibility of small coronary segments, even at low heart rates, was markedly reduced because of partial volume effects. Such observations were especially relevant in segments 8 (84.6%), 12 (76.9%), 10 (69.3%), 14 (53.8%), and 15 (38.5%) (Table 2). At moderate heart rates (60–70 bpm), visibility of even larger coronary segments was increasingly blurred by cardiac motion artifacts, for example, the middle sections of the RCA and LCX (segments 2 [55.0%] and 13 [45.0%]) (Table 2). At higher heart rates (>70 bpm), even large proximal coronary arterial segments had reduced visibility, as observed in segments 1 (87.1%), 11 (87.1%), and 6 (96.8%). However, the left main branch (segment 5) was always identified properly (100.0%) (Table 2).

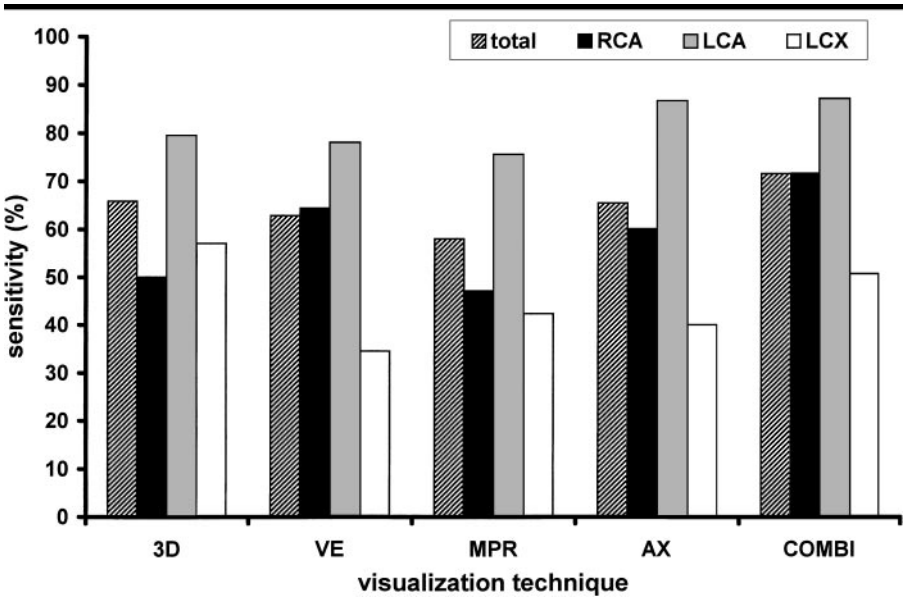

Figure 3. Bar graph shows sensitivity of CT coronary angiography in detecting atherosclerotic plaques, as well as differentiation between coronary arteries as a whole, RCA, LCA, and LCX. Three-dimensional and VE reformation, MPR, and transverse scanning *(AX)* are compared. By using a combination *(COMBI)* of all four visualization techniques, achieved sensitivity is displayed. The most sensitive results were obtained at transverse scanning (65.6%) and technique combination (71.6%). Single-vessel analysis revealed highest sensitivities for the LCA with transverse scanning (87.8%).

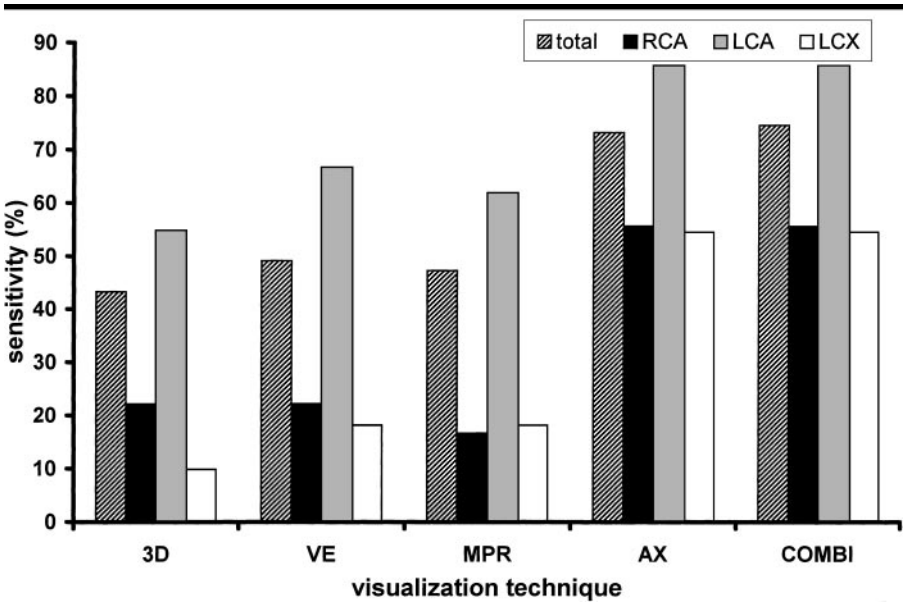

Figure 4. Bar graph shows sensitivity of CT coronary angiography in identifying HRS (>50%) and differentiating between coronary arteries as a whole, RCA, LCA, and LCX. Comparison between 3D and VE reformation, MPR, and transverse scanning *(AX)* and sensitivities achieved by combining all four visualization techniques *(COMBI)* is also displayed. The most sensitive results were obtained for transverse scanning (73.4%) and technique combination (74.7%). Single-vessel analysis revealed the highest sensitivities for the LCA with transverse scanning (85.1%).

Detection of Atherosclerotic Plaque and HRS

Atherosclerotic plaques (n = 218) were found at transverse scanning with a sen-

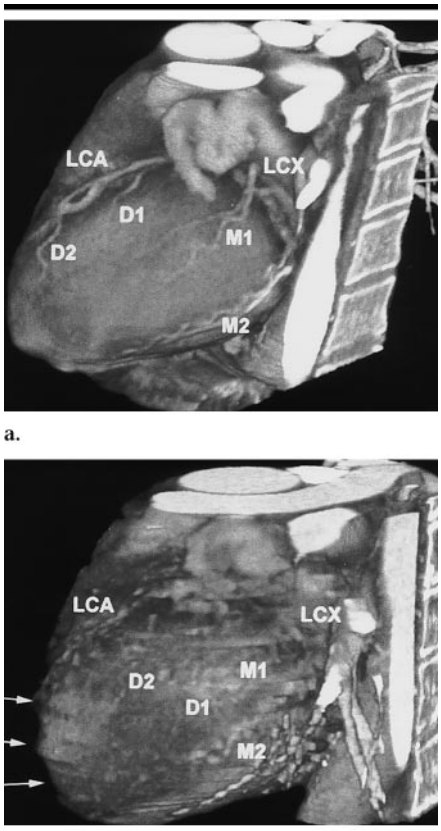

Figure 5. Three-dimensional reformations obtained after ECG-gated multi–detector row CT. Comparison between **(a)** excellent and **(b)** poor imaging techniques. **(a)** Nearly artifact-free image of left ventricle and LCAs in patient with heart rate of 56.5 bpm. Structures labeled are segment 9 (diagonal branch 1 *[D1]),* segment 10 (diagonal branch 2 *[D2]),* segment 12 (marginal branch 1 *[M1],* and segment 14 (marginal branch 2 *[M2]*). **(b)** Distinct motion artifacts in patient with elevated heart rate (70.4 bpm), in same view as **a.** Structures labeled are segment 9 (diagonal branch 1 *[D1]),* segment 10 (diagonal branch 2 *[D2]),* segment 12 (marginal branch 1 *[M1],* and segment 14 (marginal branch 2 *[M2]*). Arrows = marked motion artifacts consecutively causing nonexisting vascular discontinuance or wall irregularity.

sitivity of 65.6% (143 of 218 plaques). 3D and VE reformation showed comparably high sensitivities of 63.8% (139 of 218) and 62.4% (136 of 218), respectively, whereas the sensitivity of MPR amounted to only 58.3% (127 of 218). Specificities for the different visualization modes were transverse scanning, 93.4%; MPR, 93.2%; VE reformation, 91.4%; and 3D reformation, 95.3% (Table 3; Fig 3).

HRS (n = 79) was detected with the highest sensitivity at transverse scanning (73.4% [58 of 79 stenoses]), as compared with all other imaging techniques: VE reformation, 48.1% (38 of 79); MPR, 46.8% (37 of 79); and 3D reformation, 43.0% (34 of 79) (Table 3). Specificities of individual techniques amounted to greater than 97.7%: transverse scanning, 99.5%; 3D reformation, 97.7%; MPR, 98.2%; and VE, 98.4% (Table 3; Fig 4).

Combined interpretation of all four techniques led to sensitivity of 71.6% (156 of 218 plaques) for identification of atherosclerotic plaques and 74.7% (59 of 79 stenoses) for detection of HRS. Specificity was 95.5% for atherosclerosis and 99.3% for HRS (Table 3; Figs 3, 4).

Analysis of coronary arterial main branches (RCA, LCA, and LCX) revealed marked differences in sensitivity. In the LCA, 86.7% (85 of 98) of all atherosclerotic plaques and 85.1% (40 of 47) of all HRS could be identified at transverse scanning. Atherosclerotic plaques were also detected, with comparable results, by using all other visualization techniques: 77.6% (76 of 98 plaques) for VE reformation, 79.6% (78 of 98) for 3D reformation, and 75.5% (74 of 98) for MPR. HRS was identified with distinctly lower sensitivities: 66.0% (31 of 47 stenoses) for VE reformation, 53.2% (25 of 47) for 3D reformation, and 61.7% (29 of 47) for MPR (Table 3). Missed HRS at transverse scanning were all located in small segments 8 (n = 2), 9 (n = 4), and 10 (n = 1) (Table 4).

In the RCA, VE reformation and transverse scanning revealed atherosclerotic plaques, with sensitivities of 63.2% (36 of 57 plaques) 68.4% (39 of 57), respectively. With 3D reformation (50.1% [29 of 57] and MPR (47.4% [27 of 57), results approaching nearly 50% were obtained. HRS was identified in 28.6% (four of 14 HRS) with VE and 3D reformation, in 57.1% (eight of 14 HRS) with transverse scanning, and in 21.4% (three of 14 HRS) with MPR (Table 3). Missed HRS at transverse scanning was located in segments 1 (n = 1), 2 (n = 3), 3 (n = 1), and 4 (n = 1) (Table 4).

In the LCX, sensitivities less than 55.5% were reached for atherosclerotic plaques: VE reformation, 34.9% (22 of 63 plaques); transverse scanning, 57.1% (36 of 63); MPR, 39.7% (25 of 63); and 3D reformation, 57.1% (32 of 63). HRS was identified with sensitivities as follows: 3D reformation, 11.1% (two of 18 stenoses); VE and MPR, 22.4% each (four of 18); and transverse scanning, 55.5% (10 of 18) (Table 3). Missed HRS at transverse scanning was in segments 11 (n = 2), 12 (n = 5), 13 (n = 2), and 14 (n = 1) (Table 4).

TABLE 4
Segmental Allocation of HRS (>50%) and Missed Stenoses

Vessels and Segments	No. of Stenoses (n = 79)	No. of Missed Stenoses (n = 23)
RCA		
1	7	1
2	5	3
3	1	1
4	1	1
LM		
5	2	NA
LCA		
6	17	NA
7	15	NA
8	8	2
9	4	4
10	1	1
LCX		
11	4	2
12	7	5
13	5	2
14	2	1
15	NA	NA

Note.—NA = not applicable.

DISCUSSION

Since introduction of spiral CT as a noninvasive tool for depiction of the coronary arteries, the clinical value of both coronary calcium screening and CT coronary angiography has been subject to several studies (3,8–11). However, each new visualization technique has to compete with invasive coronary angiography, which currently represents the reference standard (12–14). Until now, results of larger studies can be drawn from only electron-beam CT. Although a significant correlation between the amount of calcium score and the degree of atherosclerotic wall changes has been demonstrated for electron-beam CT (15–20), the diagnostic value of this technique is still controversial (21). Thus, identification and segmental assignment of even high-grade calcifications alone does not inevitably deliver sufficient information concerning localization and the degree of possible stenosis (22). Furthermore, it has often been demonstrated that calcified plaques are at no higher risk of spontaneous rupture than are noncalcified plaques and thus bear no higher cardiac risk (12,23). On the contrary, it is mostly the "soft plaque," for example, noncalcified atherosclerotic plaque, that ruptures spontaneously, subsequently causing an acute cardiac incident (12,18,19,24–26). Until now, such plaques could not be sufficiently identified at electron-beam CT because of its

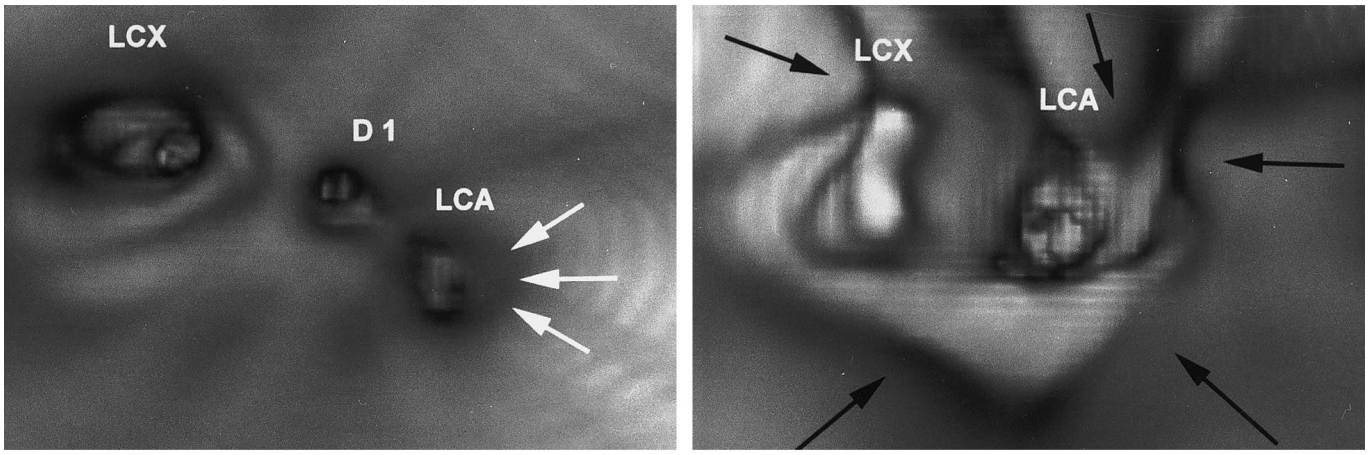

a. b.

Figure 6. VE image obtained in coronary arteries depicts left main branch to junction of LCX and LCA. Diagonal branch 1 *(D1)* also is shown. **(a)** Image obtained in patient with heart rate of 56.5 bpm provides excellent display of vascular lumen and 50% soft-plaque stenosis (arrows) of proximal LCA. **(b)** Image obtained in patient with medium heart rate (68 bpm) shows distinct motion artifacts (arrows) simulating nonexisting atherosclerosis and stenosis.

low spatial resolution (21). However, current multi–detector row CT scanners with a spatial resolution up to 9 lp/cm in plane and 6 lp/cm in the third space (8), half-second rotation times, and large volume coverage for the first time permit high-resolution CT angiography. In general, such studies are analyzed solely by means of transverse scans. Unfortunately, coronary arteries, during their epicardial and/or endocardial course, tend to spread along all three dimensions, often rendering difficult an evaluation based solely on unidirectional transverse scans. In particular, medial and distal sections of the coronary arteries may often either be displayed in an unfavorable cutting angle or be affected by partial volume effects.

CT coronary imaging revealed highest sensitivities for the detection of atherosclerotic wall changes on transverse scans. It seems that transverse scans are less susceptible to motion artifacts, while other techniques, even at low heart rates, often tend to simulate nonexisting vascular discontinuance or nonexisting wall irregularities (Figs 5–8). However, while MPR and transverse scans were evaluated on a 512 × 512 matrix, 3D and VE reformations were analyzed on only a 256 × 256 matrix. The poor results obtained for MPR may have been due to the fact that strictly orthogonal reformation could be performed only along a centerline that was previously reconstructed with VE (Figs 6, 8). Consequently, segments not captured with VE on MPRs were not displayed, either. Restrictions in software, unfortunately, did not permit higher resolution for volume-rendered objects such as 3D or VE reformations. The low sensitivity of 3D reformation demonstrates the inability of this technique to display abnormal findings on the myocardial side of the vessel (Fig 5).

The most important limitation of this study was the small number of patients and therefore the small number of stenoses. In addition, several coronary segments did not even have abnormal findings and were consequently not evaluated. With regard to invasive coronary angiography, it may be critical that for evaluation, no quantitative coronary angiography was performed. However, in the course of a retrospective study, a fair amount of data could not be evaluated with this technique. We therefore think that in the future, prospective multicenter studies may be necessary to obtain data of higher accuracy.

As compared with the invasive technique, CT angiography nevertheless showed lower sensitivity for detecting both atherosclerosis and HRS. This, in particular, was also due to the fact that image quality was not sufficient for all coronary segments and all heart rates, which was in contrast with the results of other studies (27). However, whereas in this other study only (large) proximal parts of the coronary arteries were considered, the present study included all segments equally.

Our findings concerning restrictions in visibility at elevated heart rates correspond well with the results found by other investigators (28), who have reported sufficient image quality at heart rates of only 60 bpm ± 8.

Increased motion artifacts in the medial and distal parts of the RCA and LCX, particularly at higher rates, may be due to

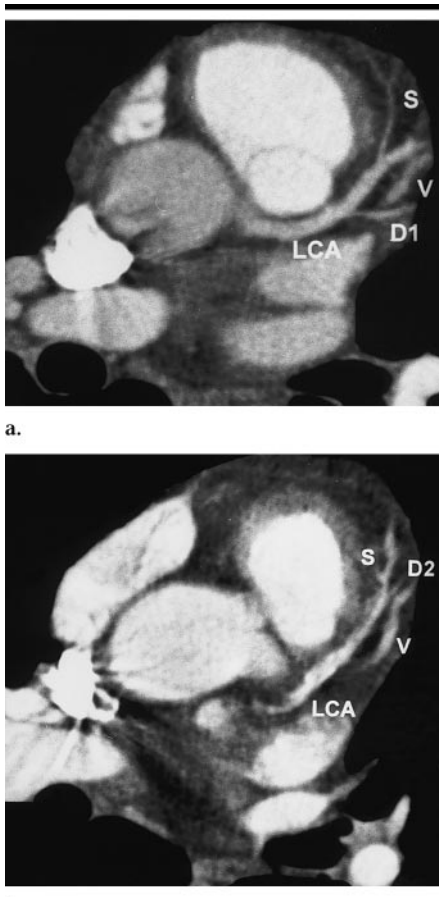

a.

b.

Figure 7. Transverse CT scans obtained at level of proximal LCA for comparison between patients with **(a)** low and **(b)** elevated heart rate. **(a)** Well differentiated vascular anatomy in patient with heart rate of 56.6 bpm. *D1* = diagonal branch 1, *S* = septal branch, *V* = cardiac vein. **(b)** Distinct motion artifacts obtained at elevated heart rate (72.2 bpm) suggest nonexisting wall irregularity and vascular stenosis. *D2* = diagonal branch 2, *S* = septal branch, and *V* = cardiac vein.

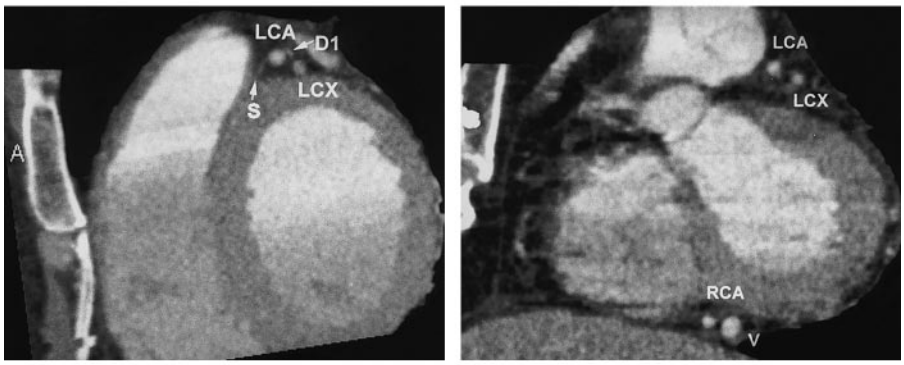

a. b.

Figure 8. MPRs (view from left side) cut orthogonally to vessel lumen for comparison between patients with **(a)** low and **(b)** elevated heart rates. **(a)** Nearly artifact-free MPR shows very small vascular structures in patient with heart rate of 56.6 bpm. *A* = anterior, *D1* = diagonal branch, *S* = septal branch. **(b)** MPR in patient with elevated heart rate (72.2 bpm) shows distinct blurring of coronary vessels. Vessels in caudal parts of heart show fewer motion artifacts because of fixation of heart at diaphragm. *V* = cardiac vein.

the close proximity of both coronary arteries to the atrium, which is activated again in the early diastolic phase. Measurements in 25 patients revealed a significantly higher proneness to motion artifacts within the RCA and LCX, as compared with the LCA (29). The diastolic acquisition window is markedly reduced and thus is the time frame for artifact-free reconstruction.

Our results display a lower in-plane and z-plane resolution than that given by technical design (1.25 mm) (4). Partial volume effects may be at least partly responsible, as previously observed at electron-beam CT (5), showing strong coherence between vascular diameter and resulting measurement error. The smaller the lumen analyzed, the higher the corresponding measurement error (5). However, such small vessels in particular significantly contributed to the low sensitivity, as demonstrated for the LCX or LCA, in which nearly all HRS was situated in only very small segments.

In conclusion, transverse scanning was the superior technique in evaluation of CT coronary angiography and showed the lowest propensity for artifacts, even at increased heart rates. Combination of all four image review methods may lead to slightly better results, but at the expense of distinctly expanded reconstruction and exploration times. Thus, in our daily routine, diagnosis in the coronary arteries is generally performed solely on transverse scans. Additional MPR is applied only in those cases and in those coronary segments that render difficult grading of stenosis on the basis of transverse scanning alone, such as in some middle sections of the coronary arteries. VE and 3D images are restricted to specific questions, for example, preoperative cardiac morphology or demonstrations to the patient.

References

1. Becker CR, Knez A, Jakobs TF. Detection and quantification of coronary artery calcifications with electron-beam and conventional CT. Eur Radiol 1999; 9:620–624.
2. Flamm SD. Coronary artery calcium screening: ready for prime time? Radiology 1998; 208:571–572.
3. Kopp AF, Ohnesorge B, Flohr T, et al. Cardiac multidetector-row CT: first clinical results of retrospectively ECG-gated spiral with optimized temporal and spatial resolution. Rofo Fortschr Geb Rontgenstr Neuen Bildgeb Verfahr 2000; 172:429–435. [German]
4. Ohnesorge B, Flohr T, Becker CR, et al. Technical aspects and applications of fast multislice cardiac CT. Medical Radiology 2000-Diagnostic Imaging, Volume Multislice CT (in press).
5. Achenbach S, Moshage W, Ropers D, Bachmann K. Comparison of vessel diameters in electron beam tomography and quantitative coronary angiography. Int J Card Imaging 1998; 14:1–7.
6. Kopp AF, Schroeder S, Kuettner A, Ohnesorge BM, Georg C, Claussen CD. Multidetector-row CT for noninvasive coronary angiography: results in 102 patients. Radiology (abstr) 2000; 217(P):375.
7. Detre KM, Wright E, Murphy ML, Takaro T. Observer agreement in evaluating coronary angiograms. Circulation 1975; 52: 979–986.
8. Becker CR, Knez A, Leber A, et al. Initial experiences with multi-slice detector spiral CT in diagnosis of arteriosclerosis of coronary vessels. Radiologe 2000; 40:118–122. [German]
9. Fischbach R, Heindel W. Detection and quantification of coronary calcification: an update. Rofo Fortschr Geb Rontgenstr Neuen Bildgeb Verfahr 2000; 172:407–414.
10. Becker CR, Ohnesorge B, Flohr T, et al. Untersuchung der koronarien mit dem mehrschicht-spiral CT. Electromedica 1999; 67:116–119.
11. Stanford W, Thompson BH. Imaging of coronary artery calcification: its importance in assessing atherosclerotic disease. Radiol Clin North Am 1999; 37:257–272.
12. Wexler L, Brundage B, Crouse J, et al. Coronary artery calcification: pathophysiology, epidemiology, imaging methods and clinical implications—a statement for health professionals from the American Heart Association Writing Group. Circulation 1996; 94:1175–1192.
13. McKeogh D, McAnulty JH. Diagnostic angiography of the coronary arteries. Semin Interv Radiol 1999; 16:102–107.
14. Scanlon PJ, Faxon DP, Audet AM. ACC/AHA guidelines for coronary angiography. J Am Coll Cardiol 1999; 33:1756–1824.
15. Budoff MJ, Georgiou D, Brody A, et al. Ultrafast computed tomography as a diagnostic modality in the detection of coronary artery disease: a multicenter study. Circulation 1996; 93:898–904.
16. Janowitz WR, Agatston AS, Viamonte M. Comparison of serial quantitative evaluation of calcified coronary artery plaque by ultrafast computed tomography in persons with and without obstructive coronary artery disease. Am J Cardiol 1991; 68:1–6.
17. Schmermund A, Baumgart D, Gorge G, et al. Coronary artery calcium in acute coronary syndromes: a comparative study of electron-beam computed tomography, coronary angiography, and intracoronary ultrasound in survivors of acute myocardial infarction and unstable angina. Circulation 1997; 96:1461–1469.
18. Agatston AS, Janowitz WR, Hildner FJ, Zusmer NR, Viamonte M, Detrano R. Quantification of coronary artery calcium using ultrafast computed tomography. J Am Coll Cardiol 1990; 15:827–832.
19. Baumgart D, Schmermund A, Goerge G, et al. Comparison of electron beam computed tomography with intracoronary ultrasound and coronary angiography for detection of coronary atherosclerosis. J Am Coll Cardiol 1997; 30:57–64.
20. Stanford W. Coronary artery calcification as an indicator of preclinical coronary artery disease. RadioGraphics 1999; 19: 1409–1419.
21. Gutfinger DE, Leung CY, Hiro T, et al. In vitro atherosclerotic plaque and calcium quantitation by intravascular ultrasound and electron-beam computed tomography. Am Heart J 1996; 131:899–906.
22. Kaufmann RB, Sheedy PF, Breen JF, et al. Detection of heart calcification with electron beam CT: interobserver and intraobserver reliability for scoring quantification. Radiology 1994; 190:347–352.
23. Cheng GC, Loree HM, Kamm RD, Fishbein MC, Lee RT. Distribution of circumferential stress in ruptured and stable atherosclerotic lesions: a structural analysis with histopathological correlation. Circulation 1993; 87:1179–1187.
24. Falk E. Plaque rupture with severe preexisting stenosis precipitating coronary

thrombosis: characteristics of coronary atherosclerotic plaques underlying fatal occlusive thrombi. Br Heart J 1983; 50: 127–134.
25. Ihling C. Pathomorphology of coronary atherosclerosis. Herz 1998; 232:69–77. [German]
26. Richardson PD, Davies MJ,Born GV. Influence of plaque configuration and stress distribution on fissuring of coronary atherosclerotic plaques. Lancet 1989; 21: 941–944.
27. Hong C, Becker C, Brüning R, Knez A, Schoepf UJ, Reiser MF. Die moeglichkeiten, limitationen und optimierung von retrospektivem EKG-gating des herzens mit einem mehrzeilen-spiral-CT. Rofo Fortschr Geb Rontgenstr Neuen Bildgeb Verfahr 2000; 2000:s172.
28. Hong C, Becker CR, Bruening RD, Schoepf UO, Knez A, Reiser MF. Retrospective ECG gating technique for reduction of cardiac motion artifacts in multi-slice CT coronary angiography (abstr). Radiology 2000; 217(P):374.
29. Achenbach S, Ropers D, Holle J, Muschiol G, Daniel WG, Moshage W. In-plane coronary arterial motion velocity: measurement with electron-beam CT. Radiology 2000; 216:457–463.